



Effects of thermal annealing on elimination of deep defects in amorphous In–Ga–Zn–O thin-film transistors



Haochun Tang^a, Keisuke Ide^a, Hidenori Hiramatsu^{a,b}, Shigenori Ueda^c, Naoki Ohashi^{b,c}, Hideya Kumomi^b, Hideo Hosono^{a,b}, Toshio Kamiya^{a,b,*}

^a Materials and Structures Laboratory, Tokyo Institute of Technology, 4259 Nagatsuta, Midori-ku, Yokohama 226-8503, Japan

^b Materials Research Center for Element Strategy, Tokyo Institute of Technology, Mailbox SE-6, 4259 Nagatsuta, Midori-ku, Yokohama 226-8503, Japan

^c National Institute for Materials Science, 1-2-1 Sengen, Tsukuba, Ibaraki 305-0047, Japan

ARTICLE INFO

Article history:

Received 2 December 2015

Received in revised form 29 February 2016

Accepted 1 March 2016

Available online 4 March 2016

Keywords:

Amorphous oxide semiconductor

Subgap states

Hard X-ray photoemission spectroscopy

Post-deposition thermal annealing

Near-valence band maximum defects

ABSTRACT

We investigated the effects of thermal annealing for high-density subgap states in amorphous In–Ga–Zn–O (a-IGZO) films by focusing on low-quality defective films deposited without O₂ supply (LQ films). It was found that most of the subgap states were thermally unstable and decreased dramatically by annealing at ≤400 °C in O₂. These defects (but with different shapes) were further reduced by 600 °C annealing, whose subgap states appeared similar to that of a-IGZO films deposited at an optimum condition (high quality, HQ films) and annealed at 300 °C. However, electron Hall mobilities and field-effect mobilities of their thin-film transistors (TFTs) were low for the LQ films/TFTs even annealed at 600 °C compared to those for the HQ films/TFTs. It implies that not only the subgap states but also heavier structural disorder deteriorated the electron transport in the LQ films. The present results also suggest that although a-IGZO deposition without O₂ supply is sometimes employed in particular for DC sputtering, supplying some O₂ gas would be better to produce good TFTs at lower temperatures.

© 2016 Elsevier B.V. All rights reserved.

1. Introduction

Since the first report of amorphous oxide semiconductor (AOS) thin-film transistors (TFTs) [1], the thin film properties, TFT characteristics, and display applications have been studied intensively because of their advantageous features such as large electron mobilities ($>10 \text{ cm}^2/(\text{V}\cdot\text{s})$), small subthreshold voltage swing (S value $<0.2 \text{ V}\cdot\text{decade}^{-1}$), and low temperature fabrication process [2,3]. In particular, amorphous In–Ga–Zn–O with the nominal chemical composition of In:Ga:Zn = 1:1:1 (a-IGZO) is now commercialized for very high-resolution liquid crystal displays (LCDs), power-saving LCDs, large-size (up to 77 in.) organic light-emitting diode displays, etc. [4–6].

Notwithstanding that IGZO TFTs are already commercialized, stability is still a critical issue (see e.g., [7–9] for positive-bias stability (PBS) and [10–13] for negative-bias illumination stress (NBIS) tests). In particular for the NBIS tests, it is recognized that the negative shift of the threshold voltage (V_{th}) is associated with the excitation of subgap photons from deep-energy defects just above the valence band maximum (near-VBM states, centered at ~2.3 eV from the conduction band (CB) edge and extends from the VBM level to ~1.5 eV towards the Fermi level (E_{F})) [14–16], which was firstly found by hard X-ray photoemission

spectroscopy (HAXPES) [17]. Our first-principles density functional theory (DFT) calculations suggest a possibility that oxygen deficiencies with free space (voids) would be a plausible origin of near-VBM states [18, 19]; while, weakly-bonded (in other words, undercoordinated) oxygen is found to form a part of near-VBM states [20] and is suggested also by beyond-DFT calculations [21–24].

Recently, Sallis and co-workers reported an unusual subgap feature observed in a-IGZO deposited with an undesirable deposition condition during film fabrication (i.e., sputtering without O₂ supply), where the near-VBM states are connected to an extra defect band that covers the whole energy region in the band gap (E_{g}) (step-wise near-CBM states) [25]. Our group also observed a similar result by employing a conventional radio-frequency magnetron sputtering (RFMS) system with the usual base pressure P_{base} of $\sim 10^{-4}$ Pa (STD sputtering) [26]. On the other hand, such step-wise near-CBM states were not detected in films deposited with a much clean ultra-high vacuum chamber (UHV sputtering with $P_{\text{base}} \sim 10^{-7}$ Pa) even if using the same undesirable deposition condition. It has been reported that the STD sputtered a-IGZO films contain high-density impurity hydrogen at $[\text{H}] > 10^{20} \text{ cm}^{-3}$ [27] while $[\text{H}]$ is reduced to $\sim 10^{19} \text{ cm}^{-3}$ by the UHV sputtering [28]. Therefore, we concluded that the residual hydrogen/H₂O in the STD deposition chamber would cause the strong reduction reaction which enhances the formation of the high-density near-CBM states as well as the near-VBM states [26].

On the other hand, post-deposition thermal annealing at 300–400 °C is usually applied to AOS TFTs to improve their performances, stability,

* Corresponding author at: Materials and Structures Laboratory, Tokyo Institute of Technology, 4259 Nagatsuta, Midori-ku, Yokohama 226-8503, Japan.

E-mail address: tkamiya@msl.titech.ac.jp (T. Kamiya).

and uniformity, a part of which would be related to the reduction of the near-VBM states [29]. The effects of different annealing temperatures (T_{ann}) in O_2 atmosphere have been investigated. For example, TFT characteristics deteriorated when $T_{\text{ann}} \geq 500^\circ\text{C}$ due to depletion of the impurity hydrogen [30]; while, re-doping of H from additional wet- O_2 annealing (addition of appropriate H_2O to O_2 [31]) at 400°C recovers the TFT characteristics, implying that some hydrogens passivate defect states [32]. In the case of the much defective a-IGZO films (low-quality (LQ) films), the densities of the subgap states are much larger than those of a-IGZO films employed for practical devices (high-quality (HQ) films), which would be associated with the poor performances of TFTs using LQ a-IGZO channels. However, there has been no systematic study on how the near-VBM states are reduced by thermal annealing.

In this work, we investigated the effects of thermal annealing on the near-VBM states in relation to film properties including optical, structural, and electrical properties. We, in particular, focused on LQ films because it is easier to see behaviors of the above defects.

2. Experimental

2.1. Film preparation

A-IGZO films were deposited on silica glass substrates at room temperature (RT) by STD RFMS using a polycrystalline InGaZnO_4 target. The growth chamber was evacuated to $P_{\text{base}} \sim 10^{-4}$ Pa. Unlike the usual deposition conditions for a-IGZO TFTs (the oxygen flow rate ratio $R_{\text{O}_2} = [\text{O}_2] / ([\text{O}_2] + [\text{Ar}]) \sim 3\%$ [33]), we mainly employed $R_{\text{O}_2} = 0$ (without O_2 supply, i.e., LQ films) so that we can observe effects of near-VBM states clearly [26]. Some films were deposited at the optimum condition of $R_{\text{O}_2} = 3\%$ (i.e., HQ films). RF power and working pressure were fixed at 70 W and 0.55 Pa, respectively. After deposition, these films were subjected to rapid thermal annealing in an O_2 atmosphere at varied $T_{\text{ann}} = 100\text{--}800^\circ\text{C}$ for 1 h.

2.2. Film properties and TFT characteristics

Structures of a-IGZO films were characterized using grazing incidence X-ray diffraction (GIXRD, using Rigaku SmartLAB) with the grazing angle of 0.5° . Film thickness and densities were extracted by analyzing X-ray reflectivity (XRR) spectra. The chemical compositions were determined by X-ray fluorescence spectroscopy (XRF, Rigaku ZSX100e) calibrated with the results of inductively-coupled plasma atomic emission spectroscopy. Optical absorption coefficient (α) spectra were obtained using the reflection correction equation $\exp(-\alpha d) = T / (1 - R)$ (where d is the film thickness, T and R are optical transmittance and reflectance measured with an ultraviolet–visible–near-infrared spectrophotometer (Hitachi U-4100)). HAXPES measurements were performed at the BL15XU undulator beamline (excitation X-ray energy: $h\nu = 5950.3$ eV) in SPring-8 [34]. Electrical properties including the Hall mobility (μ_{Hall}) and carrier concentration (N_e) were obtained by Hall effect measurements (Toyo, ResiTest 8300) using the van der Pauw configuration at RT.

Top-contact, bottom-gate structure TFTs were fabricated on thermally oxidized SiO_2 (150 nm)/ n^+ -Si substrates with the thickness ~ 40 nm and channel width/length of $300/50\ \mu\text{m}$ by photolithography and lift-off. Ti and Au (10 and 30 nm) were used as source and drain electrodes deposited sequentially by e-beam evaporation. TFT characteristics were measured with a semiconductor parameter analyzer in the dark at RT.

3. Results and discussion

3.1. Reduction of subgap states with post-deposition thermal annealing

Fig. 1 shows the α spectra of LQ films annealed at varied $T_{\text{ann}} = 200\text{--}700^\circ\text{C}$ in comparison with that of an unannealed film. We reported

that the residual impurity hydrogen would cause many effects during the film deposition, in particular without O_2 supply during deposition, which enhances the formation of oxygen deficiencies (V_O) and segregation of metallic indium (In^0) [26]. The unannealed film in Fig. 1 exhibits a long-tail subgap absorption extending from the optical E_g to the infrared region at least to 0.5 eV, which is attributed to the segregated In^0 as reported in [26]. The long-tail subgap absorption was almost unchanged up to $T_{\text{ann}} \sim 400^\circ\text{C}$, while, almost disappeared at $T_{\text{ann}} = 500\text{--}600^\circ\text{C}$.

Similar effects were observed also in HAXPES spectra. As shown in the normalized HAXPES spectra around the E_g region (Fig. 2(a), where the intensities are normalized by the O 2p peak in the VB spectra), the high-density subgap states including the near-VBM states (from VBM to ~ 1.5 eV towards CBM) and step-wise near-CBM states (from ~ 2.0 eV to E_F) were detected for the unannealed and 200°C annealed films, while were reduced significantly from $T_{\text{ann}} = 300^\circ\text{C}$. In particular, after annealed at 400°C , the peak-shape near-VBM states decreased significantly, and only shoulder-shape near-VBM states (the energy range is similar to the peak-shape near-VBM states, but the spectrum shape is different) remained by 600°C annealing. Further, the step-wise near-CBM states were annihilated due to the oxidation of segregated In^0 ; while, the peak-shape near-CBM states appeared below E_F extending to ~ 2.5 eV, whose states are the same as those observed in HQ a-IGZO films deposited at optimum O_2 supply condition [15,16,26]. Further increasing T_{ann} to 800°C further decreased the shoulder-shape near-VBM states, which would be explained that crystallization reduced the subgap defects. These results indicate that most of the subgap states introduced by $R_{\text{O}_2} = 0$ deposition (peak-shape near-VBM states and step-wise near-CBM states) are thermally unstable and annihilated by low- T annealing even at 300°C .

Fig. 2(b) shows the estimated subgap density of states (DOSs) extracted from Fig. 2(a). It is difficult to estimate the absolute values of DOSs in PES spectra because each signal state has different photo-ionization cross sections (S_p). Here we employed a rough but simple estimation method; assume that the S_p value of the subgap states is the same as that of the O 2p states that constitute the VB states. We can calculate the density of the O 2p electrons from the film density obtained by XRR and the chemical composition measured by XRF, and then convert the peak area ratio between the O 2p states and the subgap states to the density of trapped electron. In Fig. 2(b), the subgap states were separated into two regions; (i) near-VBM states from VBM to 2 eV towards CBM, and (ii) In^0 (step-wise near-CBM) states from 2 eV to CBM. It clearly shows that the high-density subgap states decrease sharply at $T_{\text{ann}} \sim 300^\circ\text{C}$.

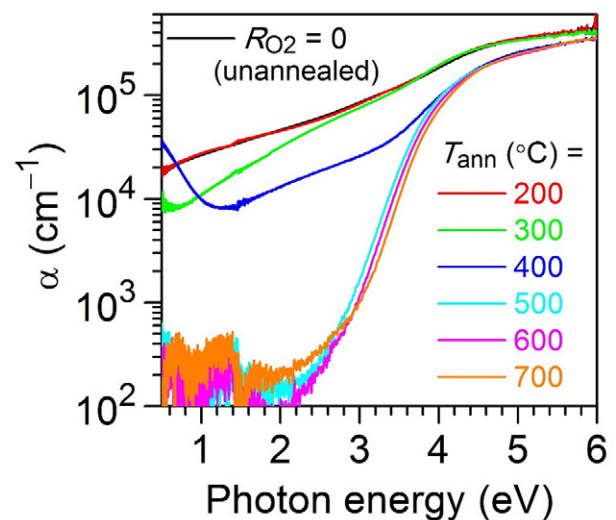


Fig. 1. Optical absorption (α) spectra of the LQ $R_{\text{O}_2} = 0$ films unannealed and annealed at varied $T_{\text{ann}} = 200\text{--}700^\circ\text{C}$. The long-tail subgap absorption is primarily attributed to the segregated In^0 .

Download English Version:

<https://daneshyari.com/en/article/1663789>

Download Persian Version:

<https://daneshyari.com/article/1663789>

[Daneshyari.com](https://daneshyari.com)